Late Quaternary aeolian dynamics, pedostratigraphy and soil formation in the North European Lowlands – new findings from the Baruther ice-marginal valley

Florian Hirsch[1], Roland Spröte[2], Thomas Fischer[3], Steven L. Forman[4], Thomas Raab[1], Oliver Bens[5], Anna Schneider[1], Reinhard F. Hüttl[2,5]

[1] Brandenburg University of Technology Cottbus – Senftenberg (BTU), Chair of Geopedology and Landscape Development, Germany, P.O. Box101344, 03013 Cottbus, Germany

[2] Brandenburg University of Technology Cottbus – Senftenberg (BTU), Chair of Soil Protection and Recultivation

[3] Brandenburg University of Technology Cottbus – Senftenberg (BTU), Central Analytical Laboratory, Germany, thomas.fischer@b-tu.de

[4] Baylor University, Department of Geology, Geoluminescence Dating Research Lab, Waco, Texas, USA

[5] Helmholtz-Centre Potsdam German Research Center for Geosciences (GFZ), Germany

Abstract

The formation of dunes in central Europe reflects ample sediment supply during the last deglacial hemicycle. A Quaternary inland dune complex in southern Brandenburg, Germany, was studied to frame the duration of pedogenesis in two outcrops containing buried paleosols. An integrative approach, which combined geomorphological, sedimentological, pedological and chronological methods was used to identify aeolian deposition events, ensuing pedogenesis and anthropogenic remobilization. At the outcrops, which were situated approximately 2 km apart from each other, a total of twelve samples of the aeolian sands were dated using optically stimulated luminescence (OSL) and a further six samples using 14C dating. Although the dunes have similar morphological features, these forms have a different history of aeolian sand deposition and pedogenesis. At the older dune (Gl 1) the surface soil is a well developed Podzol, whereas soil development of the younger dune (Gl 2) is clearly in an initial state. The studied sites of the dune complex also differ in grain size distribution and in the presence of buried soils, thereby indicating a climatic impact on aeolian remobilization.

Zusammenfassung

Die Bildung von Dünen in Mitteleuropa ist in der Regel das Ergebnis äolischer Prozesse während des Spätquartärs. Im Rahmen dieser Studie wurde der Zeitraum von Bodenentwicklungsphasen in einem spätquartären Dünenkomplex in Südbrandenburg untersucht, in dem zwei Paläoböden aufgeschlossen sind. Mit Hilfe eines integrativen Ansatzes aus geomorphologischen, sedimentologischen und bodenkundlichen Verfahren sollen in Verbindung mit Absolutdatierungen Phasen der äolischen Dynamik und der Bodenentwicklung sowie anthropogene Landschaftseingriffe chronologisch eingegrenzt werden. Hierfür wurden an zwei Aufschlüssen, die etwa zwei Kilometer voneinander entfernt sind, zwölf Datierungen mittels optisch stimulierter Lumineszenz (OSL) an äolischen Sanden durchgeführt. Des Weiteren wurden sechs 14C Datierungen an organischem Material, das in den Sanden gefunden wurde, durchgeführt. Obwohl die beiden untersuchten Dünen zum selben Dünenkomplex gehören, kann mittels der durchgeführten Untersuchungen eine ältere (Gl 1) und eine jüngere (Gl 2) Düne unterschieden werden. Während auf der älteren Düne Gl 1 ein ausgeprägter Podsol zu finden ist, belegt ein initialer Boden das jüngere Alter von Gl 2. Zudem weisen Unterschiede in der Textur und in der Stratigraphie der Dünen auf eine unterschiedliche Genese der beiden Standorte.

Late Quaternary aeolian dynamics, pedostratigraphy and soil formation in the North European Lowlands – new findings from the Baruther ice-marginal valley

1. Introduction

The landscape in the northern European lowlands, including the main parts of northern Germany, was formed by periglacial and glacial processes during the cold stages of the Late Pleistocene. The maximum ice advance during the last ice age is assumed to be approx. 21 to 22 ka with the so called Brandenburg stage (*Litt* et al. 2007; *Ehlers* et al. 2011), whereas *Lüthgens* et al. (2010) dated the Brandenburg stages on glaciofluvial sediments between 34 ka to 24 ka and *Heine* et al. (2009) dated the Brandenburg ice advance using cosmogenic in situ [10]Be on erratic blocks to 20-19 [10]Be ka BP.

In the extraglacial area and with the retreat of the glaciers, the cold climate and lack of a dense vegetation cover enabled aeolian processes in the sandy substrates which led to the generation of dunes and the formation of so called coversands. In this European Sand Belt (*Koster* 1988; *Zeeberg* 1998; *Koster* 2009) numerous studies, including dating, have been conducted, e.g. in the Netherlands (*Bateman* and *Van Huissteden* 1999; *Kasse* 2002; *Vandenberghe* 2013), in northern Germany (*Alisch* 1995; *Bussemer* et al. 1998; *Kaiser* et al. 2006), Poland (*Kozarski* and *Nowaczyk* 1991; *Hirsch* et al. 2015) and Russia (*Kalińska-Nartiša* 2015). Several phases of aeolian activity can be distinguished in the European Sand Belt with 28-18 ka, 18-14 ka and 13-10 ka (*Kasse* 2002), as well as 25-20 ka and 15-12 ka (*Vandenberghe* 2013), respectively. A short stabilization of the landscape during the lateglacial led to the formation of the so-called Usselo soil and Finow soil (*Kaiser* et al. 2009). The Usselo soil formed in sandy substrates during the Allerød and is characterized by high charcoal amounts consisting mainly of pine, the enrichment of organic material and podzolic bleaching, whereas the development of the Finow soil is dominated by brunification and weathering (*Schlaak* 1998; *Kaiser* et al. 2009). Both soils are found fossilized by younger aeolian deposits in wide areas of the European Sand Belt and, therefore, suggest similar climatic conditions during the lateglacial. However, the pedogenic character of the Finow soil has recently been challenged (*Jankowski* 2012).

With the onset of the Holocene, the succession of vegetation stabilized the landscape. During the Holocene, several studies prove a further reshaping by aeolian processes due to human induced changes in vegetation. In eastern Brandenburg, a tilled topsoil dated with ^{14}C of charcoal ranging from 1294-1076 cal BP to 960-765 cal BP, is buried under a 2 m thick aeolian deposit (*Raab* et al. 2015). *Küster* et al. (2014) proved aeolian shaping of the landscape since the 13th century in Mecklenburg-West Pomerania triggered by landuse. In the Baruther ice-marginal valley anthropogenic influences were reported by *Baray* and *Zöller* (1993), *De Boer* (1995) and *Hilgers* (2007). *Baray* and *Zöller* (1993) dated dune sediments with embedded Meso- to Neolithic flint fragments (*Hilgers* 2007), and *De Boer* (1995) described ceramics, dated to the 12th and 13th century. *Hilgers* (2007) discussed the relation between human impact and dune reactivation in the Holocene. In an earlier study, a 1.5 m buried Podzol adjacent to our outcrop Glashütte 2 was dated to 1100 ± 500 a BP by thermoluminescence (TL), and to 1490 ± 70 ^{14}C yr (1530-1290 cal BP) by ^{14}C dating of the fossilized topsoil (*De Boer* 1995). A ^{14}C dating on charcoal from the Finow soil at Glashütte yielded an age of 13240-12070 cal BP (*Kaiser* et al. 2009).

Due to the fact that earlier investigations on the Late Quaternary landscape development of the Baruther Ice-marginal valley were based on a few datings of several disturbed outcrops only, we focussed on two sites with a small scale screening. An integrative approach, which combined geomorphological, sedimentological, pedological and chronological methods is presented in this study to (I) extend the chronological findings on Late Quaternary morphodynamics of the Glashütte site from earlier studies (*Baray* and *Zöller* 1994; *De Boer* 1995; *Hilgers* 2007; *Kaiser* et al. 2009) and (II) to chronologically narrow the anthropogenic remobilization of the aoelian deposits.

2. Study site

The study site is situated on a dune complex in the Baruther Ice-marginal valley to the southwest of the terminal moraine of the Brandenburg ice advance. Therefore, the study site was affected by periglacial and glaciofluvial processes during the Late Pleistocene with a aeolian relocation of the sandy substrate (*Fig. 1*). Two stratigraphic sections were logged and sampled for OSL and ^{14}C dating and associated soil analyses. Soil pit Gl 1 (UTM: 33U E401140 N 5765677) is located at the road cut of the dune north of Klasdorf (*Fig. 1*). Here, the dune has a height of 12 m (*Photo 1*). At soil profile Gl 2 (UTM 33U E399211 N5766506) the dune has a height of 5.6 m (*Photo 2*).

Late Quaternary aeolian dynamics, pedostratigraphy and soil formation in the North European Lowlands – new findings from the Baruther ice-marginal valley
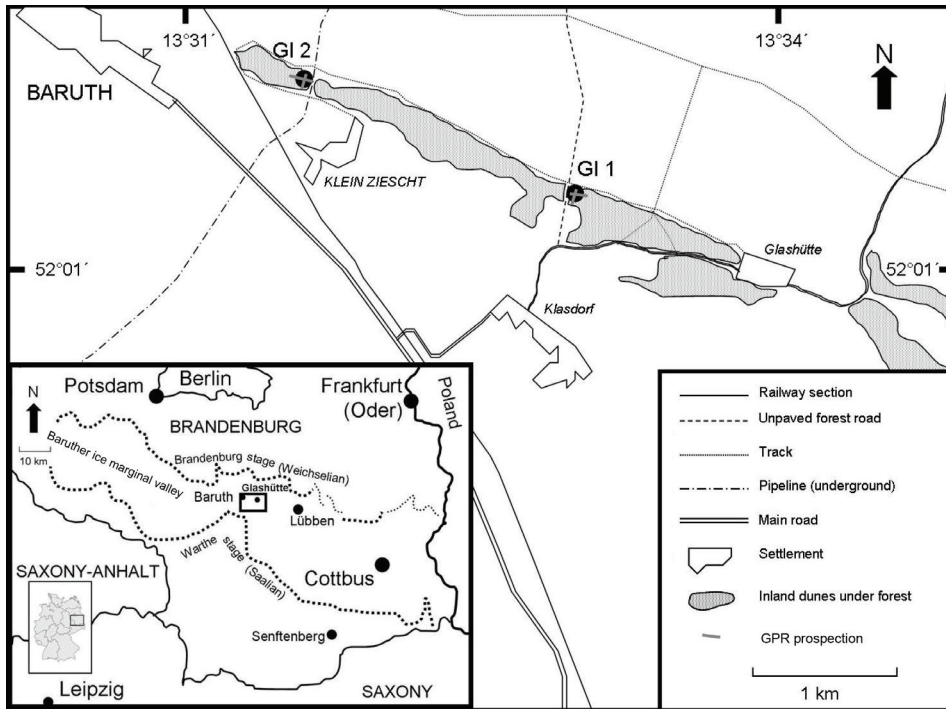

Fig 1   Location map of the study site in the Baruther ice-marginal valley between Baruth and Glashütte in Brandenburg, Germany and the dune complex with the two study sites Glashütte 1 (Gl 1) (near Glashütte) and Glashütte 2 (Gl 2) (own elaboration)

Photo 1   Study site Glashütte 1 (see car left in the picture for scale, photo: T. Raab)

Photo 2   Study site Glashütte 2 (photo: T. Raab)

2.1 Climate and Vegetation

At present, the climate in southern Brandenburg is transitional between oceanic and continental. The mean annual rainfall is 520 mm and the mean annual air temperature is 8.5 °C (data from meteorological station Baruth, period 1961-1990). The landscape at the study site is dominated by meadows and pastures. Currently, the dunes are covered with pine forests and birch areas at its northern fringe. Pollen spectra indicated that prior to pervasive human impact on this landscape in the 12th century the sandy dunes were dominated by alder. Before the 12th century, pollen analysis proved that mainly alder (*Alnus*), pine (*Pinus*), birch (*Betula*) and heath (*Calluna vulgaris*) dominated (*De Boer* 1995). According to *Usinger* (2004), the typical vegetation type in the Baruther Ice-marginal valley was open pine forest.

2.2 Geomorphology and Pedology

According to *Marcinek* (1961), the Baruther Ice-marginal valley is subdivided into several ice-marginal terrace levels: The "Oldest Baruther Ice-marginal valley" (maximum extent of Weichselian ice sheet near Baruth, 75-60 m a.s.l.; *Juschus* 2003), the "Older Baruther Ice-marginal valley" (63-55 m a.s.l.), the "Younger Baruther Ice-marginal valley" terrace (55-50 m a.s.l.) and the "Youngest Baruther Ice-marginal valley" (< 50 m a.s.l.). The inland dunes, the focus of our research, overlay the deposits of the "Older Baruth Ice-marginal valley" level at 57-60 m a.s.l. (*De Boer* 1995).

The dunes around the village of Glashütte are part of a broad dune complex covering wide areas in the Baruther ice-marginal valley, and are classified at Glashütte as longitudinal but also as small, 100 m wide, parabolic dunes extending 300 m in a W to E-direction. The maximum height of this dune complex is 71 m a.s.l. (*De Boer* 1995). The height of dunes in the Glashütte area is 25 m above the dune base. Dune morphology indicates a paleowinds transport direction from the west and south (*De Boer* 1995). *Kadar* (1938) classified the dunes based on morphostratigraphy, which was differentiated amongst linear, longitudinal and parabolic dunes. An earlier assessment based on morphology of depositional and blow-out areas infer westerly winds for accretion of dunes south of Baruth (*Lembke* 1939). The Brandenburg inland dunes consist of nearly pure quartz sand (*Gellert* and *Scholz* 1970).

Soils in the Baruther Ice-marginal valley north and south of the inland dunes are mainly peat and gleyic soils developed under the influence of ground water (LBGR 2001). Soils of the sandy dunes are Arenosols with podzolic features (LBGR 2001). Buried soils in the dunes are Regosols (*De Boer* 1995) and Podzols (*De Boer* 1995; *Hilgers* 2007). In addition, south of the dunes in glaciofluvial or fluvial sands gleyic soils with Cambisol features mainly prevail with the occasional occurrence of podzolic features (LBGR 2001).

3. Material and Methods

3.1 Soil analysis

At Gl 1 (from top to 4.0 m) and at Gl 2 (from top to 4.6 m) profiles were excavated to classify soil horizons and soil types, to take samples for laboratory analyses, and for dating. Soil horizons were described in the field according to the German Soil Taxonomy (*Ad-hoc AG Boden* 2005) and classified following the *IUSS Working Group WRB* (2014) and *FAO* (2006). Fifteen soil samples from Gl 1 (*Table 1*) and eighteen soil samples from Gl 2 (*Table 1*) were taken for laboratory analyses. The samples were dried at 40 °C and then sieved with a mesh <2 mm to separate gravel from the fine soil. Only the fine soil was used for laboratory analyses.

Soil pH was measured in water suspension (soil:H_2O = 1:2.5) and soil organic carbon concentration (C_T) was determined by dry combustion using an Elemental Analyser (Elementar Vario EL). Grain-size distribution is analyzed by wet sieving and fractionation according to DIN ISO 11277 (pipette method) on 20 g of samples, after humus destruction and dispersion with sodium pyrophosphate. Soil color was determined with the Munsell Soil Color Charts. Concentrations of oxalate and dithionite iron fractions (Fe_o and Fe_d) were determined according to the method described by *Schlichting* et al. (1995).

3.2 GPR

Ground Penetrating Radar (GPR) measurements were carried out in cross-sections and along the ridges of both dunes in order to extrapolate the information on soil horizon depth from the profiles and to characterize the internal sedimentary structure of the dunes. A RAMAC/GPR System (MALÅGeoscience, Sweden) with 500 MHz shielded antennae

Glashütte 1 · Glashütte 2

Late Quaternary aeolian dynamics, pedostratigraphy and soil formation in the North European Lowlands – new findings from the Baruther ice-marginal valley

Table 1 Soil chemistry and texture at Glashütte 1 and Glashütte 2

Glashütte 1

Depth (cm)	Horizon Ad-hoc AG Boden (2005)	Horizon FAO (2006)	Colour (Munsell)	C_T (in %)	pH (H2O)	Fed (mg/kg)	Feo (mg/kg)	Feo/Fed	coarse sand	medium sand	fine sand	silt	clay	Texture (Ad-hoc AG Boden) 2005
0 - 35	Ahe	E	7.5YR 6/2	0.4	4.5	554	361	0.65	1.8	46.9	49.9	0.7	0.6	fSms
35 - 50	Bms	Bsm	8.75YR 5.5/6	0.7	4.3	1464	1138	0.78	1.9	46.7	50.3	0.5	0.6	fSms
50 - 90	iICv	C	10YR6/6	0.2	4.4	354	175	0.49	0.6	33.8	65.1	0.1	0.4	fSms
90 - 130	iICv	C	10YR6/6	0.2	4.5	382	209	0.55	0.7	24.8	73.9	0.2	0.3	fSms
130 - 170	iICv	C	10YR6/6	0.1	4.4	246	215	0.87	1.1	35.0	63.2	0.2	0.4	fSms
170 - 200	iICv	C	10YR6/6	0.1	4.5	292	127	0.44	3.5	57.8	38.2	0.1	0.5	mSfs
200 - 230	iICv	C	10YR6/6	0.1	4.6	280	134	0.48	16.7	50.1	33.0	0.2	0.0	mSfs
230 - 270	iICv	C	10YR6/6	0.1	4.6	307	121	0.39	3.7	40.1	56.0	0.1	0.2	fSms
270 - 300	iICv	C	10YR6/6	0.1	4.5	352	127	0.36	2.1	41.3	56.4	0.1	0.1	fSms
300 - 310	iICv	C	10YR6/6	0.2	4.4	537	197	0.37	1.4	28.1	69.5	0.6	0.4	fSms
310 - 330	iICv	C	2.5Y 5/6	0.2	4.5	537	181	0.34	2.5	33.9	62.6	0.5	0.5	fSms
330 - 332	II fBsv	2Bswb1	10 YR 7/3 and 7.5 YR 5/6	0.8	4.3	1867	1146	0.61	6.7	51.1	35.4	2.0	4.9	mSfs
332 - 340	II fBsv	2Bswb2	2.5Y 5/6	0.6	4.4	1034	720	0.70	8.7	53.8	35.1	1.0	1.3	mSfs
340 - 360	III fAhe	3Eb	2.5Y 5/3	0.2	6.6	332	122	0.37	5.6	48.5	45.0	0.4	0.4	mSfs
360 - 400	III iICv	3C	10YR 7.5/4	0.1	4.7	437	180	0.41	6.0	52.5	41.2	0.1	0.2	mSfs

Glashütte 2

Depth (cm)	Horizon Ad-hoc AG Boden (2005)	Horizon FAO (2006)	Colour (Munsell)	C_T (in %)	pH (H2O)	Fed (mg/kg)	Feo (mg/kg)	Feo/Fed	coarse sand	medium sand	fine sand	silt	clay	Texture (Ad-hoc AG Boden) 2005
0 - 5	Ah	Ah	2.5Y 4/2	1.3	4.4	582	341	0.59	0.9	39.9	57.0	0.5	1.7	fSms
5 - 25	M	C	2.5Y 5/3	0.4	4.5	448	215	0.48	1.1	49.4	48.0	0.2	1.3	fSms
25 - 50	M	C	10YR 5/4	0.3	4.5	446	206	0.46	0.8	42.9	55.1	0.1	1.2	fSms
50 - 75	M	C	10YR 6/4	0.2	4.4	444	203	0.46	0.7	41.1	57.3	0.1	0.7	fSms
75 - 100	M	C	10YR 5/4	0.2	4.6	427	211	0.50	1.6	40.4	57.2	0.1	0.7	fSms
100 - 125	M	C	10YR 5/4	0.2	4.5	375	182	0.48	5.2	60.2	33.7	0.1	0.8	mSfs
125 - 150	M	C	2.5Y 5/4	0.2	4.5	435	221	0.51	0.7	47.4	50.6	0.2	1.1	fSms
150 - 200	M	C	10YR 5/4	0.2	4.6	414	234	0.56	1.1	53.1	45.3	0.2	0.3	mSfs
200 - 220	M	C	10YR 5/6	0.2	4.4	442	269	0.61	1.1	42.6	55.5	0.2	0.8	fSms
220 - 250	M	C	2.5Y 5/4	0.2	4.4	398	207	0.52	1.9	49.1	48.2	0.1	0.7	mSfs
250 - 300	M	C	10YR 5/4	0.2	4.6	369	226	0.61	2.3	45.8	51.1	0.1	0.7	fSms
300 - 330	M	C	2.5Y 5/4	0.2	4.5	432	248	0.57	1.5	41.2	56.4	0.2	0.7	fSms
330 - 360	M	C	2.5Y 5/4	0.3	4.5	380	227	0.60	1.4	40.6	56.3	0.2	1.5	fSms
360 - 362	II fAh	2Eb1	10YR 3/1	1.2	4.7	435	286	0.66	1.7	43.3	50.6	2.8	1.7	fSms
362 - 369	II fAe	2Eb2	10YR 5/2	0.3	4.9	159	121	0.76	1.9	48.8	47.7	0.8	0.7	mSfs
369 - 384	II Bs	2Bsb1	10YR 4/6	0.6	4.3	854	754	0.88	1.1	49.1	48.4	0.4	1.1	mSfs
384 - 410	II Bs	2Bsb3	10YR 5/6	0.2	4.7	505	243	0.48	1.3	47.3	50.5	0.2	0.6	fSms
410 - 460	II iICv	2C	10YR 5/4	0.2	4.6	339	157	0.46	1.7	47.7	49.8	0.1	0.7	fSms

was used in a common-offset antenna configuration. Reflection data was gathered continuously in order to reach a small measurement step size. Data were processed in ReflexW (Sandmeier Scientific Software) by interpolating the trace spacing to 10 cm intervals; applying a dewow, bandpass filtering and background removal to reduce noise; phase correction for aligning the groundwave signal; an exponential gain to increase signal amplitudes in lower parts of the profile; and fk-migration to reduce diffractions. The electromagnetic wave propagation velocity was determined by an interactive velocity adaptation based on diffraction hyperbolae in the radargrams.

3.3 Radiocarbon dating

Three charcoal fragments at Gl 1 and two at Gl 2 were sampled for AMS-^{14}C dating by the AMS-C14 Laboratory Erlangen. Calendar correction of radiocarbon dates was done using OxCal 4.2 (*Bronk Ramsey* 2009) in combination with the Intcal13 calibration curve (*Reimer* et al. 2013). The radiocarbon calendar corrected time scales is from the reference year AD 1950, whereas OSL ages are from the reference year AD 2000.

3.4 Luminescence dating

The SAR protocols were applied to quartz grains usually from primary dune bedforms (*Murray* and *Wintle* 2003). Equivalent doses were determined on the 150-250 µm quartz fraction for 30 aliquots. Each aliquot contains ~1,000 to 500 quartz grains affixed to an approx. 2 mm diameter area on aluminum discs. Aeolian sands are mineralogically mature with an SiO_2 content of >90 %. The quartz fraction was isolated by density separations using the heavy liquid Na-polytungstate, and a subsequent 40-minute immersion in HF to etch the outer ~10 µm of grains, which are affected by alpha radiation (*Mejdahl* and *Christiansen* 1994). The quartz grains were rinsed finally in HCl to remove any insoluble fluorides. The purity of the quartz separate was evaluated by petrographic inspection and point counting of a representative aliquot. Samples that showed >1 % of non-quartz minerals were retreated with HF and rechecked petrographically. The purity of the quartz separates was also tested by exposing aliquots to infrared excitation (1.08 watts from a laser diode at 845 ± 4 nm), which preferentially excites feldspar minerals. Samples measured showed weak emissions (<300 counts/second), at or close to background counts with infrared excitation, and a ratio of emissions from blue to infrared excitation of >20, indicating a spectrally pure quartz extract (cf. *Duller* et al. 2003).

An Automated Risø TL/OSL-DA-15 system (*Bøtter-Jensen* et al. 2000) was used for SAR analyses. Blue light excitation (470 ± 20 nm) from an array of 30 light-emitting diodes delivered ~15 mW/cm^2 to the sample position at 90 % power. A Thorn EMI 9235 QA photomultiplier tube coupled with three 3 mm-thick Hoya U-340 detection filters, transmitting between 290 nm and 370 nm, measured photon emissions. Laboratory irradiations used a calibrated ^{90}Sr/^{90}Y beta source coupled with the Risø reader. All SAR emissions were integrated over the first 0.8 s of stimulation out of 50 s of measurement, with background based on emissions for the last ten second interval. The luminescence emission for quartz sands showed a dominance of a fast component (cf. *Murray* and *Wintle* 2003) with >95 % diminution of luminescence after 4 seconds of excitation with blue light.

A series of experiments was performed to evaluate the effect of preheating at 180 °C, 200 °C, 220 °C, and 240 °C on thermal transfer of the regenerative signal prior to the application of SAR dating protocols (*Murray* and *Wintle* 2003). These experiments showed no preheat-based sensitivity changes and a preheat at 220 °C was used in SAR analyses. A test for dose reproducibility was also performed following procedures of *Murray* and *Wintle* (2003) with the initial and final regenerative dose of ~ 4 grays yielding concordant luminescence response (at one sigma errors) (*Fig. 2a, 3a*).

Only aliquots with recycling ratios between 0.9 and 1.1 were retained in age calculations indicating a minimal change in the sensitivity correction through the SAR dating protocols. SAR ages are calculated by the central age model (*Galbraith* et al. 1999) because of the log normal distribution of equivalent dose (*Fig. 2b, 3b*). Optical ages are reported in years prior to AD 2000 (*Table 2*).

A dose recovery test was carried out by solar resetting a set of nine aliquots of sample UIC2184 using 80 second blue diode exposure, giving the aliquots a known beta dose (4.88 Gy) and then using the SAR procedure (using a test dose of 4.1 Gy). All ten aliquots yielded equivalent doses that overlap at two sigma with the known dose, using a 220 °C preheat, indicating that the SAR protocols are appropriate
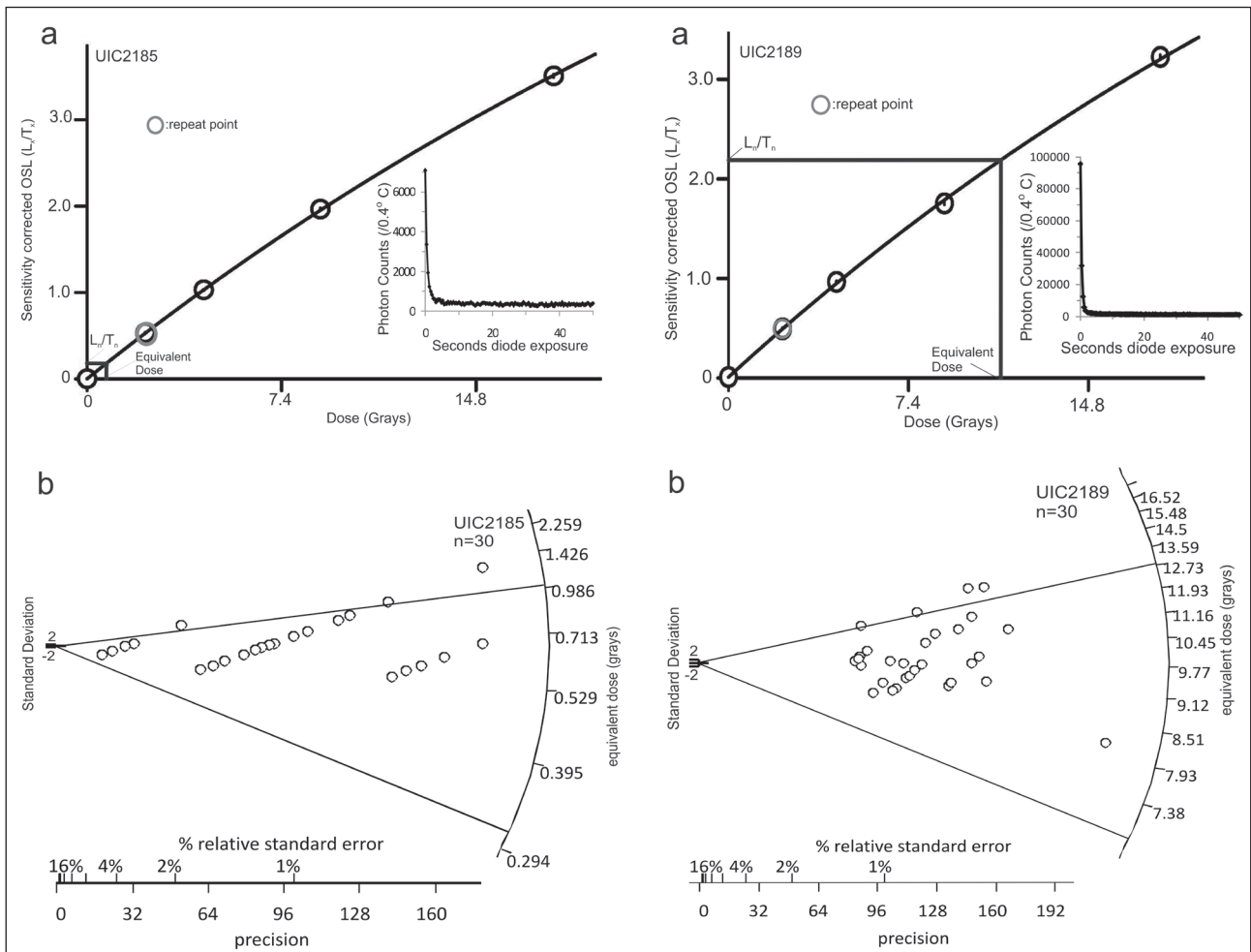
Fig. 2 a: Luminescence data for the 150-250 micron quartz aliquots for sample UIC2185 Optical decay curve measured using blue emitting diodes (470 ± 20 nm) for natural luminescence (inset) and dose response curve
b: Radial plot of equivalent dose data as in (a); lines forming the wedge indicates 2 sigma limit

Fig. 3 a: Luminescence data for the 150-250 micron quartz aliquots for sample UIC2189 Optical decay curve measured using blue emitting diodes (470 ± 20 nm) for natural luminescence (inset) and dose response curve
b: Radial plot of equivalent dose data as in (a); lines forming the wedge indicates 2 sigma limit

Table 2   Radiocarbon dating

Site	laboratory code	sample depth below surface	14C BP	cal BP	δ¹³C (0/00)
Glashütte 1	Erl-11617	90 cm	11,768 ± 75	13,749-13456	-23,8
Glashütte 1	Erl-11618	300-310 cm	10,260 ± 66	12,381-11760	-24
Glashütte 1	Erl-11619	340-360 cm	11,610 ± 72	13,571-13296	-25,2
Glashütte 2	Erl-11790	70 cm	882 ± 45	917-706	-23,6
Glashütte 2	Erl-11791	340 cm	1006 ± 38	981-796	-22,7
Glashütte 2	Erl-11792	367 cm	1954 ± 40	1990-1824	-22,3

for recovering an unknown dose (*Fig. 4*). The results of tests of samples to recycle a given dose within SAR measurement sequence, and the extent of recuperation during the dose recovery test indicates efficaciousness for preheat temperatures up to 240 °C.
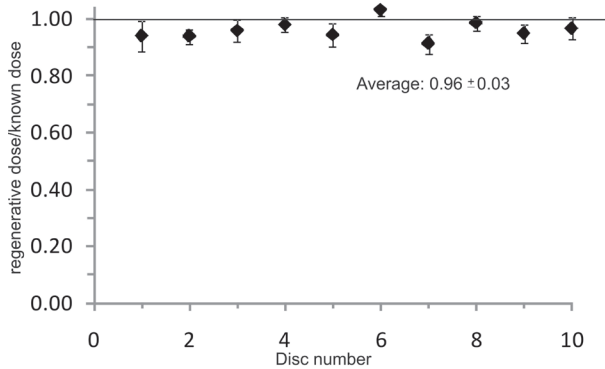

Fig. 4   Dose recovery test for UIC2184 with an applied dose of 4.4 Gy. Ratio of regenerative dose to applied dose is near unity (0.96 ± 0.3), indicating that SAR protocols accurately recover the applied dose

A determination of the environmental dose rate is needed to render an optical age. This dose rate is an estimate of sediment exposure to ionizing radiation from U and Th decay series, ^{40}K, and cosmic sources during the burial period (*Table 2*). The U and Th content of the dose rate samples, assuming secular equilibrium in the decay series and ^{40}K, were determined by inductively coupled plasma-mass spectrometry (ICP-MS) analyzed by Activation Laboratory LTD, Ontario, Canada. The beta and gamma doses were adjusted according to grain diameter (150-250 μm) to compensate for mass attenuation (0.876 beta, 0.999 gamma, *Fain* et al. 1999). A small cosmic ray component between 0.21 and 0.12 ± 0.02 mGy/yr depending on depth of sediment was included in the estimated dose rate (*Prescott* and *Hutton* 1994). A moisture content (by weight) of 5 ± 2 % was assumed reflecting current conditions.

4. Results

4.1 Stratigraphy and Pedology

At Gl 1 the upper sediment of the dune has a thickness of 330 cm with a high content of medium and fine sand (*Table 1*). At the depth of 200-300 cm the sediment is clearly stratified and has a higher content of coarse sand at a depth of 200-230 cm. A sharp change in texture and colour indicate a sedimentological change 330 cm to 332 cm below the surface. From 332-400

cm the texture of the substrate is again dominated by fine and medium sand and the sediment has cross bedding structures (*Photo 3*).
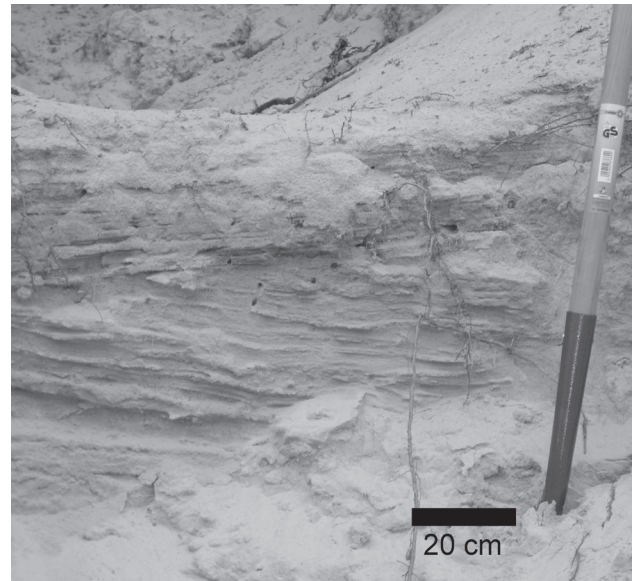

Photo 3 Cross bedding structures as an indicator for different wind directions of sand transport at Gl 1

At the top of the dune a Podzol with an 35 cm thick eluvial horizon has developed (*Fig. 5*). The eluvial horizon has a pinkish gray colour with a C_T content of 0.7 % (Ahe). The illuvial horizon below has a yellow to brownish color and is strongly cemented by sesquioxides (Bms). The parent material has a single-grain-structure, containing rusty patches along root channels and some charcoal fragments (ilCv). Between 330-360 cm a sequence of fossilized soil horizons with a strong brown to very pale brown horizon on top (330-340 cm, II fBsv), and below a greyish horizon with podzolic bleaching from 340-360 cm (III fAhe) prevails. The II fBsv is enriched with charcoal fragments, resulting in C_T values between 0.6 % to 0.8 % and higher Fe_o and Fe_d contents than below (*Table 1*). The III fAhe is also rich in finely dispersed charcoal fragments, slightly mottled, slightly humic, and has a C_T content of 0.2 %. Although this horizon has features of podzolic bleaching, the acidity of pH 6.6 is the highest in the profile (*Table 1*), with all other values ranging from 4.3 to 4.7 pH, underlining the fossil character of this eluvial horizon.

Thus, the dune at Gl 1 site exposes a stratigraphy of an Albic Rustic Ortsteinic Podzol (Arenic) over a joint occurence of a buried Finow soil (II fBsv) over an Usselo soil (III fAhe) at 350 cm below the surface. According to the German Soil Taxonomy the soil horizons in the outcrop are classified as Ahe/Bms/ilCv/II fBsv/III fAhe/III ilCv.
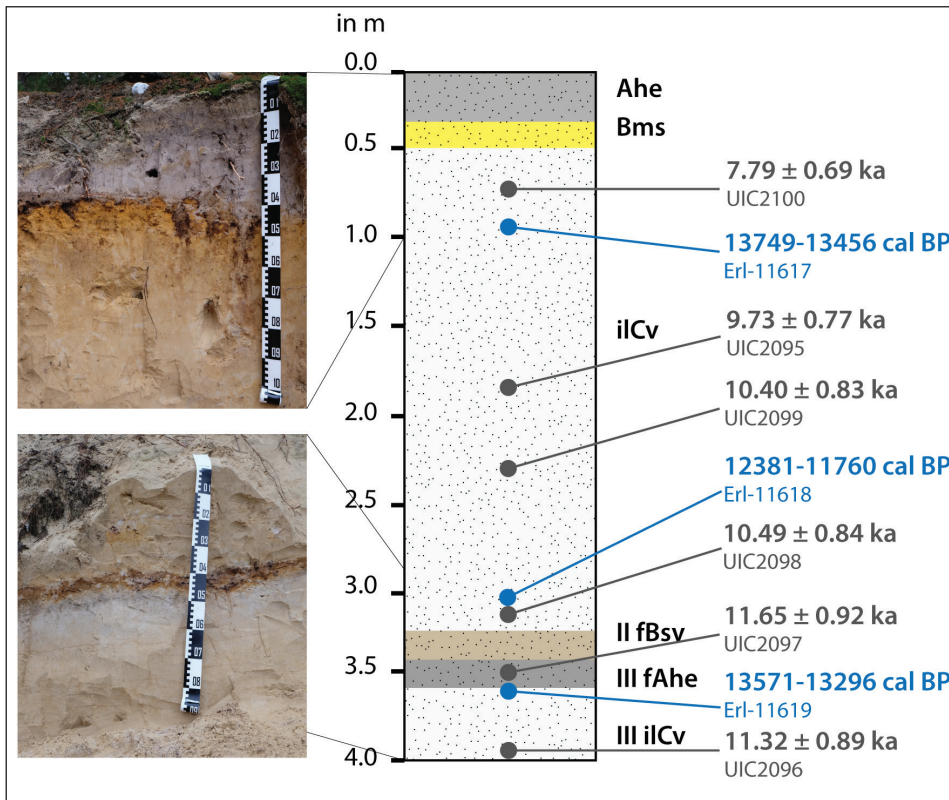
Fig. 5
Schematic stratigraphic section of Glashütte 1 with OSL- and radiocarbon dating

in m

0.0

Ahe
Bms

0.5

7.79 ± 0.69 ka
UIC2100

1.0

13749-13456 cal BP
Erl-11617

1.5

ilCv   **9.73 ± 0.77 ka**
UIC2095

2.0

10.40 ± 0.83 ka
UIC2099

2.5

12381-11760 cal BP
Erl-11618

10.49 ± 0.84 ka
UIC2098

3.0

11.65 ± 0.92 ka
UIC2097

3.5   II fBsv

III fAhe   **13571-13296 cal BP**
Erl-11619

III ilCv   **11.32 ± 0.89 ka**
UIC2096

4.0
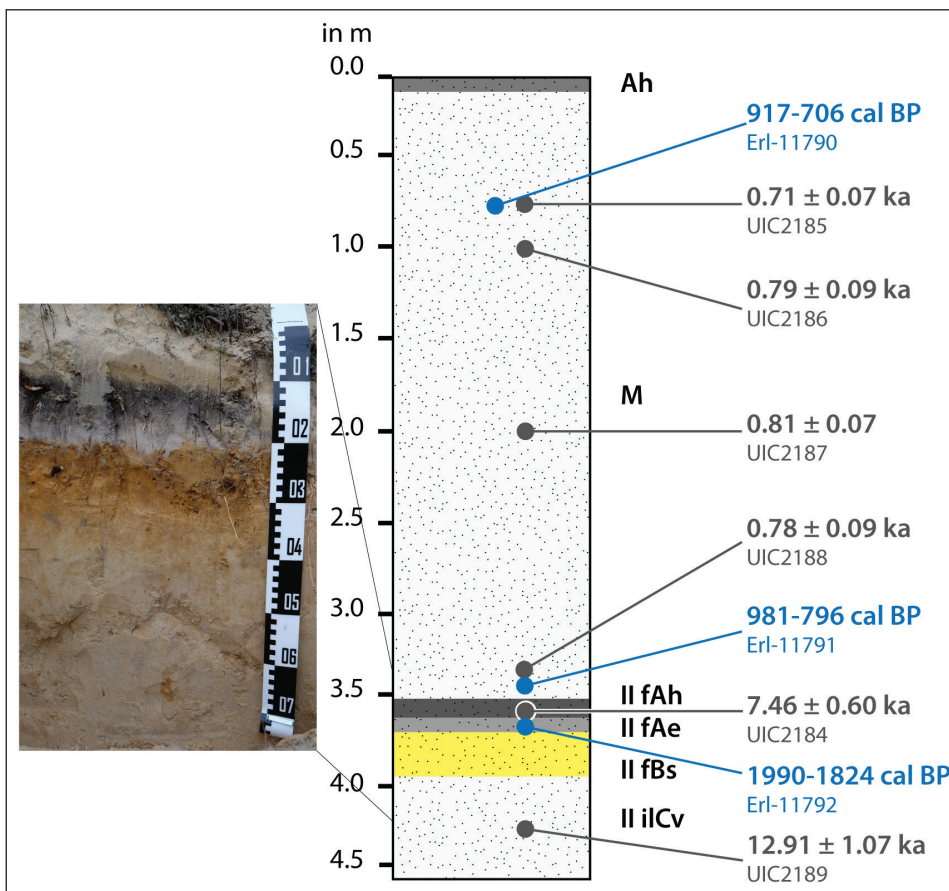
Fig. 6
Schematic stratigraphic section of Glashütte 2 with OSL- and radiocarbon dating

in m

0.0

Ah

917-706 cal BP
Erl-11790

0.5

0.71 ± 0.07 ka
UIC2185

1.0

0.79 ± 0.09 ka
UIC2186

1.5

M

2.0   **0.81 ± 0.07**
UIC2187

2.5

0.78 ± 0.09 ka
UIC2188

3.0

981-796 cal BP
Erl-11791

3.5   II fAh

II fAe   **7.46 ± 0.60 ka**
UIC2184

II fBs   **1990-1824 cal BP**
Erl-11792

4.0

II ilCv   **12.91 ± 1.07 ka**
UIC2189

4.5

Two sediments clearly separated by a fossilized soil at 360 cm below the surface are exposed in the 460 cm deep outcrop at Gl 2 (*Table 1*). Both sediments have a sandy texture dominated by high contents of medium and fine sand. A 5 cm thick Ah with a weak development constitutes the recent topsoil at surface. Here, the content of C_T is at a maximum of 1.3%. The upper deposit on top of the fossilized Podzol clearly differs from the sediment below with its homogenous yellowish brown to light olive brown color, single-grain-structured, slightly hydromorphic, and slightly humic sand (M). The fossilized II fAh has a thickness of 2 cm (*Fig. 6*). This horizon is composed of grayish sand with single-grain structure and with high amounts of finely distributed charcoal. The upper and lower limits of the II fAh are diffuse. The C_T content is high (1.2 %). The horizon below has a thickness of 7 cm and is white-gray, bleached sand with single-grain structure and high amounts of finely distributed charcoal (II fAe). Soil acidity is pH 4.9 and the content of C_T is 0.3 %. In 369-384 cm the subsoil is characterized by reddish-brown, mottled sand, with low to moderate humic accumulations along root channels, which contains finely distributed charcoal (II fBs). The C_T concentrations and the amount of Fe_d and Fe_o are higher than in the horizon above. The base of the outcrop (384-460 cm) consists of brown sand with a single-grain structure, and slightly rusty-patches along root channels and bedding structures (II ilCv). Soil stratigraphy in the 460 deep outcrop at Gl 2 is an Arenosol (Aeolic, Colluvic, Protospodic) over an Entic Rustic Podzol (Arenic), according to the German Soil Taxonomy the soil horizons are classified as Ah/M/II fAh/II fAe/II fBs/II ilCv.

Comparing the properties of sites Gl 1 and Gl 2, at both sites medium and fine sand (> 95 %) dominate the texture of the fine soil (*Table 1*). The distribution of grain size classes at Gl 1 is heterogenous, at Gl 2 the distribution is rather homogenous. At both sites podzolization is the dominating pedogenic process.

4.2 GPR

Based on several strong diffraction hyperbolae in the radargrams, which most probably result from larger roots crossed by the GPR transects, an electromagnetic wave propagation velocity of 0.12 m ns^{-1} was determined. The velocity is characteristic for the sandy dune sediments, which were moderately wet at the time of measurement (e.g., *Davis* and *Annan* 1989).

Because soil profiles were located at very steep flanks of the dunes, they could not be directly crossed in the GPR transects, so that it is not possible to precisely relate GPR signals with depths of soil horizons as observed in the profiles. Nevertheless, GPR transects reflect the basic profile stratigraphy (*Fig. 7*). All radargrams show a rapid decrease of signal amplitudes and only weak and discontinuous reflections in the uppermost meters of the profiles, which can be regarded as characteristic for the relatively homogeneous aeolian sands. At depths of up to 4 m, sets of relatively strong and continuous reflections appear in all the transects.

At location Gl 1, several strong and continuous reflections with different inclinations occur close to the location of the soil profile, ranging from a depth of about 2.5 m below the surface to the maximum recorded depth of about 4 m. In parts of the transect, two sets of reflections with different angles of inclinations can be distinguished, which can be interpreted as signals of the palaeosols and the coarser sand layer with cross-bedding structures. In the cross-section GPR transect, the stratigraphic boundary could only be observed for parts of the profile due to the limited signal penetration depth. In these parts of the profile, reflections were weak and discontinuous throughout the profile depth, probably indicating a relatively homogeneous sediment layer. In the transect along the dune ridge, the higher-amplitude reflections occur only discontinuously and do not allow for a clear interpretation of stratigraphy.

At location Gl 2, only one set of stronger reflections was observed below the signals reflecting the dune sediments. These reflections, which most probably mark the fossilized soil recorded in the profile, are running almost horizontally over the dune cross-section and can be traced over about 40 m along the dune ridge, where they are running more or less parallel to the recent dune surface. At the southern slope of the dune, the signal ends at the recent surface, which can be interpreted as a sign of an erosional truncation of the older dune surface (*Fig. 7*).
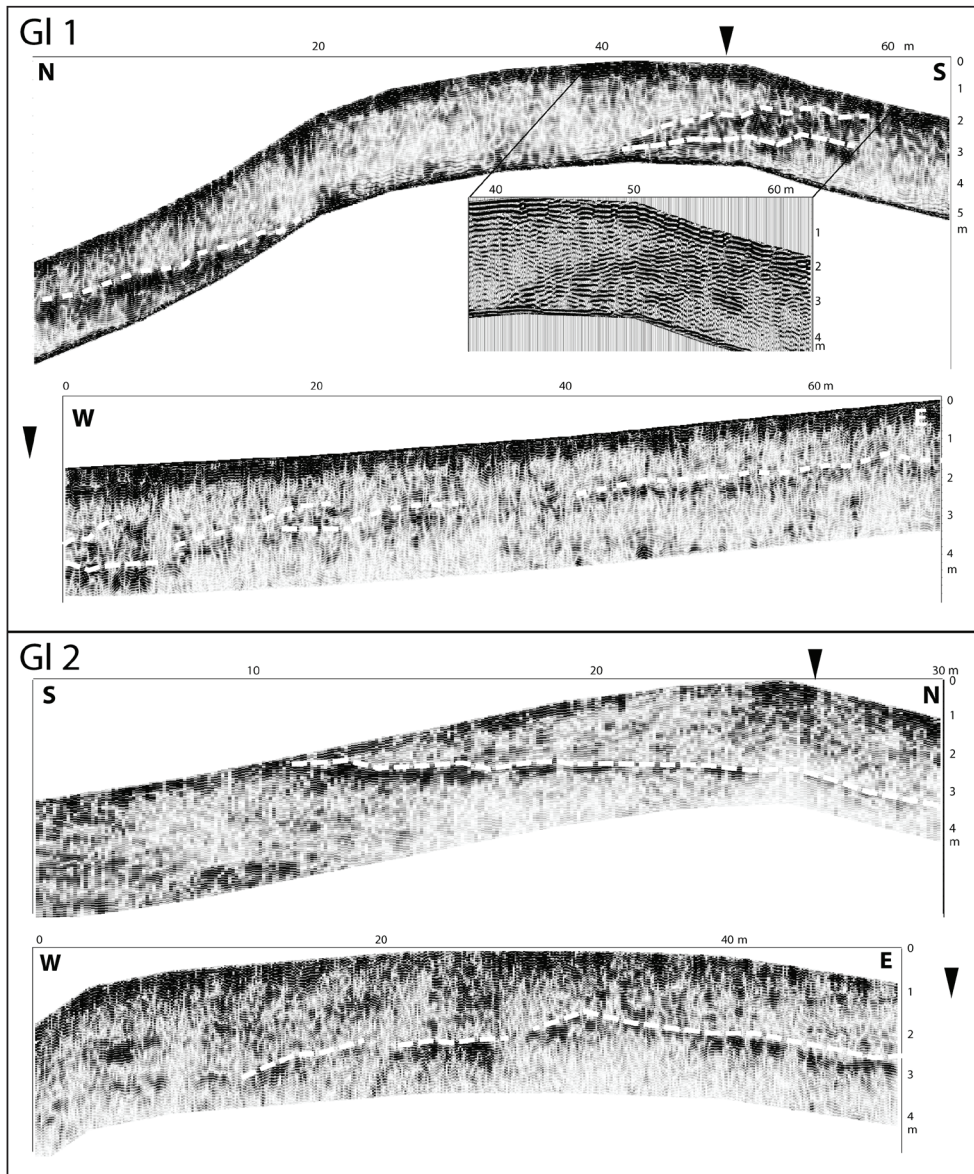
Fig. 7   GPR transects along dune cross-profiles (N-S/S-N) and ridges (W-E) at sites Glashütte 1 and 2. Depths are calculated from two-way travel times based on an electromagnetic wave velocity of 0.12 m/ns. Locations of soil profiles are roughly indicated by black arrows, but profiles were not directly crossed by GPR. Dashed lines mark the positions of distinct reflections, indicating the fossilized soils or other stratigraphical boundaries.

4.3 Luminescence and radiocarbon dating

At Gl 1 (*Fig. 5* and *Table 3*) the lower most aeolian sand yielded OSL ages of 11.3 ka ± 0.9 (UIC2096) and 11.7 ka ± 0.9 (UIC2097), the Finow soil and the sediment on top of the Finow soil have ages of 10.5 ka ± 0.8 (UIC2098) and 10.4 ka ± 0.8 (UIC2099). An age inversion with 7.8 ka ± 0.7 (UIC2100) at 180 cm below the surface and 9.7 ka ± 0.8 (UIC2095) at 70 cm depth is probably associated with erroneous sampling.

The sands at G 2 (*Fig. 6* and *Table 3*) returned four OSL ages of the upper deposit with around 0.7 ka to 0.8 ka.

The fossilized deposit has an OSL age at 365 cm of 7.5 ka ± 0.6 (UIC2084) and at the base of the outcrop the sand has an OSL age of 12.1 ka ± 1.1 (UIC2089).

At Gl 1 (*Fig. 5* and *Table 3*) all three radiocarbon datings show a Late Pleistocene age, whereas at Gl 2 all samples are of Late Holocene age (*Fig. 6* and *Table 3*). The Late Pleistocene age of the charcoal in the uppermost sediment at Gl 1 indicates the origin of the uppermost sediment as a locally reworked deposit of older substrate. Considering the sample confounding at Gl 1 at both sites the luminescence ages are stratigraphically consistent and are in general agreement with the associated ^{14}C ages.

Table 3   OSL dating

	Laboratory number	Depth (cm)	aliquots	Equivalent dose (Gray)[a]	U (ppm)[b]	Th (ppm)[b]	K$_2$O (%)[b]	Cosmic dose (mGray/yr)[c]	Dose rate (mGray/yr)[d]	OSL age (yr)[e]
Glashütte 1 Glashütte 1 OSL1[e]	UIC2095	70	30	9.07 ± 0.66	0.3 ± 0.1	1.0 ± 0.1	0.69 ± 0.01	0.19 ± 0.02	0.93 ± 0.05	**9730 ± 765**
Glashütte 1 OSL4[e]	UIC2100	180	30	6.83 ± 0.54	0.3 ± 0.1	0.8 ± 0.1	0.67 ± 0.01	0.16 ± 0.02	0.88 ± 0.05	**7790 ± 690**
Glashütte 1 OSL5	UIC2099	230	20	9.79 ± 0.75	0.5 ± 0.1	1.2 ± 0.1	0.67 ± 0.01	0.16 ± 0.02	0.94 ± 0.05	**10,400 ± 830**
Glashütte 1 OSL7	UIC2098	320	30	9.39 ± 0.67	0.3 ± 0.1	0.9 ± 0.1	0.71 ± 0.01	0.14 ± 0.01	0.90 ± 0.05	**10,490 ± 840**
Glashütte 1 OSL9	UIC2097	350	30	9.94 ± 0.71	0.4 ± 0.1	1.0 ± 0.1	0.64 ± 0.01	0.13 ± 0.01	0.85 ± 0.05	**11,650 ± 915**
Glashütte 1 OSL10	UIC2096	390	30	10.05 ± 0.72	0.4 ± 0.1	1.0 ± 0.1	0.69 ± 0.01	0.13 ± 0.01	0.90 ± 0.05	**11,320 ± 890**
Glashütte 2 Glashütte 2 OSL1	UIC2185	70	30	0.64 ± 0.06	0.4 ± 0.1	1.1 ± 0.1	0.61 ± 0.01	0.19 ± 0.02	0.90 ± 0.05	**710 ± 65**
Glashütte 2 OSL3	UIC2186	100	30	0.64 ± 0.06	0.5 ± 0.1	1.1 ± 0.1	0.48 ± 0.01	0.19 ± 0.02	0.90 ± 0.05	**790 ± 90**
Glashütte 2 OSL4	UIC2187	200	30	0.73 ± 0.07	0.5 ± 0.1	1.4 ± 0.1	0.59 ± 0.01	0.16 ± 0.02	0.89 ± 0.05	**810 ± 70**
Glashütte 2 OSL6	UIC2188	340	20	0.58 ± 0.06	0.3 ± 0.1	0.9 ± 0.1	0.61 ± 0.01	0.13 ± 0.01	0.75 ± 0.04	**780 ± 90**
Glashütte 2 OSL7	UIC2184	365	30	4.60 ± 0.33	0.4 ± 0.1	0.8 ± 0.1	0.39 ± 0.01	0.13 ± 0.01	0.62 ± 0.03	**7460 ± 600**
Glashütte 2 OSL8	UIC2189	425	30	10.39 ± 0.77	0.3 ± 0.1	0.9 ± 0.1	0.63 ± 0.01	0.12 ± 0.02	0.80 ± 0.04	**12,905 ± 1065**

[a] Quartz fraction analyzed with blue-light excitation (514 ± 20 nm) of quartz component by single aliquot regeneration protocol (*Murray* and *Wintle* 2003). Ages calculated using the central age model of *Galbraith* et al. (1999).

[b] U, Th and K$_2$O content analyzed by inductively coupled plasma-mass spectrometry analyzed by Activation Laboratory LTD, Ontario, Canada.

[c] From *Prescott* and *Hutton* 1994.

[d] Includes a moisture content of 5 ± 2%, except for UIC2188 with a moisture content of 10 ± 3%.

[f] All errors are at 1 sigma and ages from the reference year AD 2000.

[e] samples interchanged during sampling

5. Discussion

Although at both sites the dunes have a similar morphology, our results prove two chronologically different types of formation. Both dunes consist of moderately to well sorted sands, often with grain sizes between 50 μm and 70 μm (*Pye* and *Tsoar* 1990). *Alisch* (1995) studied inland dunes in northern Germany and found that these dunes are composed of 75-90 % fine sand and medium sand. The soil profiles Gl 1 and Gl 2 contain mostly medium and fine sand (> 95 %). Hence, the analysis of the grain size classes shows a grain size distribution typical for inland dunes. The dominance of fine and medium sand is similar to previously studied inland dunes (*De Boer* 1995; *Kaiser* et al. 2009). The distribution of grain size classes at Gl 1 is heterogeneous, whereas at Gl 2 the particle size distribution is more homogenous (*Table 1*). This difference in particle size distribution may reflect local and short-distance aeolian sand transport from different wind directions (*De Boer* 1990) and from different sources to the part of the dune recorded at Gl 1. The different wind directions are not only visible by the heterogenous grain size distribution at Gl 1, but also by the morphology of the dune (*Photo 1*) and the cross-bedding of the deposited sand (*Photo 3*). The sediments at Gl 2, in contrast, are most probably deposited sands which were transported solely from one wind direction.

The interpretation of more homogeneous conditions at Gl 2 is supported by GPR signals, which show only one major stratigraphic boundary dividing two units with almost no observable internal sedimentary structure. More heterogeneous grain-size distribution and internal cross-bedding structures are observable for parts of the GPR transects at Gl 1. However, GPR data for Gl 1 also indicate the deposition of several meters of relatively homogeneous sediment in parts of the dune.

The increase of silt and clay in the II fBsv at Gl 1 and in the II fAh at Gl 2 is remarkable, though confined to 2 cm vertically in the paleosol. However, it is not certain whether this increase in fines reflects in situ weathering and new mineral formation indicated by the increased Feo/Fed of the II fBsv or a downward translocation of silt and clay particles indicated by the grain size analyses. A genetic breakdown of the thin Finow soil and Usselo is not alone provable with our soil chemical and grain size analyses. Although the pedogenic character of the Finow soil is questioned

(*Jankowski* 2012) we found with our pedological investigations no indications that the Finow soil at Gl 1 represents only a sedimentological unit without pedological features. The stratigraphy with the Usselo below the Finow soil indicate an older age for the formation of the Usselo soil, but the variance in the datings taken on top and below the Usselo and Finow soil at G1 overlap. The ages at Gl 1 suggest that the sediment at the base of the outcrop with OSL ages of 11.3 ka ± 0.9 (UIC2096) and 11.7 ka ± 0.9 (UIC2097) are about 2000 years younger than the Usselo soil that formed during the Allerød (*Kaiser* et al. 2009). However, the ^{14}C dating on the charcoal with 13571-13296 cal BP (Erl-11619) is more representative for the age of the fossilized soil, because soil moisture is crucial for the calculation of OSL ages and the 5 % assumed in our calculation might be too high for the sandy substrate. However, both ^{14}C datings with 13749-13456 cal BP and 123851-11760 cal BP (Erl-11617 and Erl-11618) in the uppermost sediment of Gl 1 indicate older ages, compared with the OSL datings of the same sediment with ages ranging from 7790 ± 690 yr to 10,490 ± 840 yr (UIC 2095 and UIC 2098), which indicates the admixture of older charcoal during the formation of the younger deposit. Furthermore, the OSL dating from the Finow soil with 10,490 ± 840 yr, compared with the OSL age of the Usselo soil of 11,650 ± 915 yr (UIC 2097) suggests a younger age of the sediment where the Finow soil had developed. The OSL ages from *Hilgers* (2007) near the outcrop Gl 1 are similar to the OSL-dating from Gl 1 in this study. *Hilgers* (2007) dated the upper part of the dune to 12.65 - 13.90 ka, whereas the buried Finow soil was dated to 13.00 ± 0.94 ka (fossil Bv horizon). Consequently, an age >13.94 ka was expected for the fossil Ae horizon, indicating ongoing deposition during soil formation. However, this fAe horizon was dated to 12.76 ± 0.95 ka.

The Podzol at the surface at Gl 1, therefore, represents the podzolization during the Holocene. Although the eluvial horizon has a single grain fabric and is, therefore, prone to erosion, we found no indication for truncation of the Podzol. The thickness of the eluvial and illuvial horizons at Gl 1 is in clear contrast with Gl 2, where the minor thickness of the fossilized Podzol and the weakly podzolized topsoil are remarkable. The homogenous deposits fossilizing the Podzol are interpreted as the correlate sediment of soil erosion which is underpinned by the four young OSL ages (*Fig. 5* and *Tables 2* and *3*) ranging between 710 ± 65 yr BP (UIC 2175) to 810 ± 70 yr BP (UIC 2187) and the erosional truncation of the palaeosoil reflected

in the GPR cross-section. Furthermore, thermoluminescence dating of a sediment about 170 m apart from location Gl 2 by *Baray* and *Zöller* (1994) showed ages of 0.4 ± 0.4 kyr (Q) and 1.1 ± 0.5 kyr (F), affirming the findings of *De Boer* (1995) and *Hilgers* (2007) about the aeolian and human activities at the study site during the Late Holocene.

The time difference between the ^{14}C dating at a depth of 365 cm with 1990-1824 cal BP (Erl 11792) and the OSL dating at a depth of 365 cm of 7460 ± 600 yr BP (UIC 2184) in Gl 2 either suggest insufficient bleaching of the OSL dated quartz grains or the admixture of the sediment with younger organic, respectively pyrogenic, material which biased the radiocarbon dating. At the base of Gl 2 our OSL dating of 12,905 ± 1065 a BP shows, within the error margins, a good correlation with the TL ages of 12.4 ± 2.6 ka (Q) and 11.4 ± 3.2 ka (F) of *Baray* and *Zöller* (1994) and with 14,23 ± 0,54 ka BP of *Hilgers* (2007).

6. Conclusion

This study shows that both dune systems – even though they are just approximately 2 km apart and have similar morphological features such as height, width, and orientation – have a different history in aeolian sand deposition and pedogenesis. At dune Gl 1 the surface soil is a well developed Podzol. In contrast, dune Gl 2 soil development is clearly in an initial state showing modest accumulation of soil organic matter and weaker podzolization morphologies. The Finow soil and the Usselo soil were observed at Glashütte 1 indicating a short period during the end of the lateglacial where a meliorating climate enabled soil development. OSL dating revealed ages of approximately 11,65 ± 0,98 ka to 10,49 ± 0,84 ka, where the respective ^{14}C dating ages for charcoal average to 13571-13296 cal BP. Subsequently, the palaeosoilcomplex was fossilized by aeolian activity, probably continuing to the lateglacial. Again, a remobilization of the sands by aeolian activity occurred during the Late Holocene at Gl 2 at about 800 cal BP, and we associate this phase of soil erosion with the onset of the glasswork production.

References

Ad-hoc-AG Boden 2005: Bodenkundliche Kartieranleitung. – Bundesanstalt für Geowissenschaften und Rohstoffe, Hannover

Alisch, *M.* 1995: Das äolische Relief der mittleren Oberen Allerniederung (Ost-Niedersachsen); spät- und postglaziale Morphogenese, Ausdehnung und Festlegung historischer Wehsande, Sandabgrabungen und Schutzaspekte. – Kölner Geographische Arbeiten **62**

Baray, *M.* and *L. Zöller* 1993: Aspekte der Thermolumineszenz-Datierung an Spätglazial-Holozänen Dünen im Oberrheingraben und in Brandenburg. – Berliner Geographische Arbeiten **78** (1): 1-33

Baray, *M.* and *L. Zöller* 1994: Methodological Aspects of Thermoluminescence Dating of Late Glacial and Holocene Dune Sands from Brandenburg, Germany. – Quaternary Science Reviews **13**: 477-480, – doi: 10.1016/0277-3791(94)90061-2

Bateman, *M.D.* and *J. Van Huissteden* 1999: The timing of last-glacial periglacial and eolian events, Twente, eastern Netherlands. – Journal of Quaternary Science **14**: 277–283, – doi: 10.1002/(SICI)1099-1417(199905)14:3<277::AID-JQS460>3.0.CO;2-W

Bøtter-Jensen, *L., E. Bulur, G.A.T. Duller* and *A.S. Murray* 2000: Advances in luminescence instrument systems. – Radiation Measurements **32**: 523–528, – doi: 10.1016/S1350-4487(00)00039-1

Bronk Ramsey, C. 2009: Bayesian Analysis of Radiocarbon Dates. – Radiocarb. **51** (1): 337-360

Bussemer, *S., P. Gärtner* and *N. Schlaak* 1998: Stratigraphie, Stoffbestand und Reliefwirksamkeit der Flugsande im brandenburgischen Jungmoränenland. – Petermanns Geographische Mitteilungen **142**: 115-125

Davis, *J.L.* and *A.P. Annan* 1989: Ground-penetrating radar for high-resolution mapping of soil and rock stratigraphy. – Geophysical Prospecting **37**: 531-551, – doi: 10.1111/j.1365-2478.1989.tb02221.x

De Boer, W.M. 1990: Dünen im Baruther Urstromtal (Raum Luckenwalde-Baruth-Lübben) – Stand der Forschungslit-

eratur. – Biologische Studien Luckau **19**: 3-10

De Boer, W.M. 1995: Äolische Prozesse und Landschaftsformen im mittleren Baruther Urstromtal seit dem Hochglazial der Weichseleiszeit. – Berliner Geographische Arbeiten **84**

DIN ISO 112772002-08: Bodenbeschaffenheit – Bestimmung der Partikelgrößenverteilung in Mineralböden – Verfahren mittels Siebung und Sedimentation (ISO 11277:1998 + ISO 11277:1998 Corrigendum 1:2002). – Beuth

Duller G.A.T., L. Bøtter-Jensen and *A.S. Murray* 2003: Combining infrared- and green-laser stimulation sources in single-grain luminescence measurements of feldspar and quartz. – Radiation Measurements **37**: 543-550, – doi: 10.1016/S1350-4487(03)00050-7

Ehlers J., A. Grube, H.-J. Stephan and *S. Wansa* 2011: Pleistocene Glaciations of North Germany—New Results. – In: *Ehlers, J., P.L. Gibbard* and *P.D. Hughes* (eds.): Developments in Quaternary Sciences, 149-162, – doi: 10.1016/B978-0-444-53447-7.00013-1

Fain, J., S. Soumana, M. Montret, D. Miallier, T. Pilleyre and *S. Sanzelle* 1999: Luminescence and ESR dating Beta-dose attenuation for various grain shares calculated by a Monte-Carlo method. – Quaternary Science Reviews **18**: 231-234, – doi: 10.1016/s0277-3791(98)00056-0

FAO 2006: Guidelines for soil description. – Food and Agriculture Organization of the United Nations. -Rome

Galbraith, R.F., R.G. Roberts, G.M. Laslett, H. Yoshida and *J.M. Olley* 1999: Optical dating of single and multiple grains of quartz from Jinmium rock shelter, northern Australia: Part I, experimental design and statistical models. – Archaeometry **41**: 339-364, – doi: 10.1111/j.1475-4754.1999.tb00987.x

Gellert, J.F. and *E. Scholz* 1970: Geomorphologische Übersichtskarte 1:200,000. Berlin-Potsdam und Frankfurt-Eberswalde. – In: *Franz, H.-J., R., Schneider* and *E. Scholz* (eds.): Erläuterungen für die Kartenblätter Berlin-Potsdam und Frankfurt-Eberswalde. – Gotha/Leipzig: 9-45.

Heine, K., A.U. Reuther, H.U. Thieke, R. Schulz, N. Schlaak and *P.W. Kubik* 2009: Timing of Weichselian ice marginal positions in Brandenburg (northeastern Germany) using cosmogenic in situ 10Be. – Zeitschrift für Geomorphologie **53** (4): 433-454, – doi: 10.1127/0372-8854/2009/0053-0433

Hilgers, A. 2007: The chronology of Late Glacial and Holocene dune development in the northern Central European lowland reconstructed by optically stimulated luminescence (OSL) dating. – Diss. Univ. Köln

Hirsch, F., A. Schneider, A. Nicolay, M. Błaszkiewicz, J. Kordowski, A.M. Noryskiewicz, S. Tyszkowski, A. Raab and *T. Raab* 2015: Late Quaternary landscape development at the margin of the Pomeranian phase (MIS 2) near Lake Wygonin (Northern Poland). – Catena **124**: 28-44, – doi: 10.1016/j.catena.2014.08.018

IUSS Working Group WRB 2014: World reference base for soil resources 2014. World Soil Resources Reports, **106**. – FAO, Rome

Jankowski, M. 2012: Lateglacial soil paleocatena in inland-dune area of the Toruń Basin, Northern Poland. – Quaternary International **265**: 116-125, – doi: 10.1016/j.quaint.2012.02.006

Juschus, O. 2003: Das Jungmoränenland südlich von Berlin – Untersuchungen zur jungquartären Landschaftsentwicklung zwischen Unterspreewald und Nuthe. – Berliner Geographische Arbeiten **95**

Kadar, L. 1938: Die periglazialen Binnendünen des norddeutschen und polnischen Flachlandes. – Comptes-Rendus du Congr. Int. De Géographie: 167-183

Kaiser, K., A. Barthelmes, S. Czakó Pap, A. Hilgers, W. Janke, P. Kühn and *M. Theuerkauf* 2006: A Lateglacial palaeosol cover in the Altdarss area, southern Baltic Sea coast (Northeast Germany): investigations on pedology, geochronology, and botany. – Netherlands Journal of Geosciences **85** (3): 199-222, – doi: 10.1017/S0016774600021478

Kaiser, K., A. Hilgers, N. Schlaak, M. Jankowski, P. Kühn, S. Bussemer and *K. Przegietka* 2009: Palaeopedological marker horizons in northern central Europe: characteristics of Lateglacial Usselo and Finow soils. – Boreas **38** (3): 591-609, – doi: 10.1111/j.1502-3885.2008.00076.x

Kalińska-Nartiša, E., M. Nartišs, C. Thiel, J.-P. Buylaert and *A.S. Murray* 2015: Late-glacial to Holocene aeolian deposition in northeastern Europe – The timing of sedimentation at the Iisaku site (NE Estonia). – Quaternary International **357** (30): 70-81, – doi: 10.1016/j.quaint.2014.08.039.

Kasse, C. 2002: Sandy eolian deposits and environments and their relation to climate during the Last Glacial Maximum and Lateglacial in northwest and central Europe. – Progress in Physical Geography **26** (4): 507-532, – doi: 10.1191/0309133302pp350ra

Koster, E.A. 1988: Ancient and modern cold-climate eolian sand deposition: a review. – Journal of Quaternary Science **3** (1): 69-83, – doi: 10.1002/jqs.3390030109

Koster, E.A. 2009: The "European Aeolian Sand Belt": Geoconservation of drift sand landscapes. – Geoheritage **1**: 93-110, – doi: 10.1007/s12371-009-0007-8

Kozarski, S. and *B. Nowaczyk* 1991: Lithofacies variation and chronostratigraphy of Late Vistualian and Holocene phenomena in northwestern Poland. – In: *Kozarski, S.* (ed.): Late Vistualian and Holocene Aeolian phenomena in Central and Northern Europe. – Zeitschrift für Geomorphologie, Suppl.-Bd. **90**: 107-122

Küster, M., A. Fülling, K. Kaiser and *J. Ulrich* 2014: Aeolian sands and buried soils in the Mecklenburg Lake District, NE Germany: Holocene land-use history and pedo-geo-

morphic response. – Geomorphology **211**: 64-76, – doi: 10.1016/j.geomorph.2013.12.030

LBGR 2001: Bodenübersichtskarte des Landes Brandenburg 1:300.0002001. – Online available at: http://www.geo.brandenburg.de/boden/, May 2016

Lembke, H. 1939: Das Alter der norddeutschen Binnendünen. – Deutsche Geographische Blätter **42** (1-4): 87-96

Litt, T., *Behre*, K.E., *Meyer*, K.-D., *Stephan*, H.J. and S. *Wansa* 2007: Stratigraphische Begriffe für das Quartär des norddeutschen Vereisungsgebietes. – Quaternary Science Journal **56** (1/2): 7-65, – doi: 10.3285/eg.56.1-2.02

Lüthgens, C., M. Krbetschek, M. Böse and *M.C. Fuchs* 2010: Optically stimulated luminescence dating of fluvioglacial (sandur) sediments from north-eastern Germany. – Quaternary Geochronology **5** (2–3): 237-243, – doi: 10.1016/j.quageo.2009.06.007

Marcinek, J. 1961: Über die Entwicklung des Baruther Urstromtales zwischen Neiße und Fiener Bruch. – Wissenschaftliche Zeitschrift der Humboldt-Universität Berlin, Math.-Nat.-Reihe **X** (1): 13-46

Mejdahl, V. and *H.H. Christiansen* 1994: Procedures used for luminescence dating of sediments. – Quaternary Geochronology **13**: 403-406, – doi: 10.1016/0277-3791(94)90049-3

Murray, A.S. and *A.G. Wintle* 2003: The single aliquot regenerative dose protocol: potential for improvements in reliability. – Radiation Measurements **37**: 377-381, – doi: 10.1016/S1350-4487(03)00053-2

Pye, K. and *H. Tsoar* 1990: Aeolian sand and sand dunes. – London

Prescott, J.R. and *J.T. Hutton* 1994: Cosmic ray contributions to dose rates for luminescence and ESR dating: large depths and long-term time variations. – Radiation Measurements **23**: 497–500, – doi: 10.1016/1350-4487(94)90086-8

Raab, T., A. Raab, A. Nicolay, M. Takla, F. Hirsch, H. Rösler and *A. Bauriegel* 2015: Opencast mines in South Brandenburg (Germany) – archives of Late Quaternary landscape development and human-induced land use changes. – Archaeological and Anthropological Sciences: 1-14, – doi: 10.1007/s12520-015-0227-6

Reimer, P.J., E. Bard, A. Bayliss, J.W. Beck, P.G. Blackwell, C. Bronk Ramsey, C.E. Buck, H. Cheng, R.L. Edwards, M. Friedrich, P.M. Grootes, T.P. Guilderson, H. Haflidason, I. Hajdas, C. Hatté, T.J. Heaton, D.L. Hoffmann, A.G. Hogg, K.A. Hughen, K.F. Kaiser, B. Kromer, S.W. Manning, M. Niu, R.W. Reimer, D.A. Richards, E.M. Scott, J.R. Southon, R.A. Staff, C.S.M.Turney and *J. van der Plicht* 2013: IntCal13 and Marine13 Radiocarbon Age Calibration Curves 0–50,000 Years cal BP. – Radiocarb. **55** (4): 1869-1887

Schlaak, N. 1998: Der Finowboden – Zeugnis einer begrabenen weichselspätglazialen Oberfläche in den Dünengebieten Nordostbrandenburgs. – Münchner Geographische Abhandlungen **49**: 143-148.

Schlichting, E., H.-P. Blume and *K. Stahr* 1995: Bodenkundliches Praktikum (2nd Edition). – Berlin/Wien)

Usinger, H. 2004: Vegetation and climate of the lowlands of northern Central Europe and adjacent areas around the Younger Dryas – Preboreal transition – with special emphasis on the Preboreal oscillation. – In: *Terberger, T.* and *B.V. Eriksen* (eds.): Hunters in a changing world. – Internationale Archäologie-Arbeitsgemeinschaft, Tagung, Symposium, Kongress **5**: 1-26

Vandenberghe, D.A.G., C. Derese, C. Kasse and *P. Van den Haute* 2013: Late Weichselian (fluvio-)aeolian sediments and Holocene drift-sands of the classic type locality in Twente (E Netherlands): a high-resolution dating study using optically stimulated luminescence. – Quaternary Science Reviews **68**: 96-113, – doi: 10.1016/j.quascirev.2013.02.009

Zeeberg, J. 1998: The European sand belt in eastern Europe – and comparison of Late Glacial dune orientation with GCM simulation results. – Boreas **27**: 127-139, – doi: 10.1111/j.1502-3885.1998.tb00873.x